Generation of a 160-GHz transform-limited pedestal-free pulse train through multiwave mixing compression of a dual-frequency beat signal

S. Pitois, J. Fatome, and G. Millot

Laboratoire de Physique de l'Université de Bourgogne, 9 Avenue A. Savary, B.P. 47 870, 21078 Dijon, France

Received May 7, 2002

We report the experimental generation of a 160-GHz picosecond pulse train at 1550 nm, using multiple four-wave mixing temporal compression of an initial dual-frequency beat signal in the anomalous-dispersion regime of a nonzero dispersion-shifted fiber. Complete intensity and phase characterizations of the pulse train were carried out by means of a frequency-resolved optical gating technique, showing that 1.27-ps transform-limited pedestal-free Gaussian pulses were generated. © 2002 Optical Society of America

OCIS codes: 190.4370, 190.4380, 320.5520, 320.7100.

In the context of rapidly growing traffic in long-haul fiber transmission systems, the development of ultrashort-pulse generators that make possible high repetition rates and pulse profiles of high quality will play a crucial role in the performance of time-division-multiplexed communication systems.[1] Since current electronics-based and direct modulation technologies do not permit the generation of pulses at a repetition rate higher than 40 GHz, the nonlinear transformation of a dual-frequency signal in an optical fiber is an attractive method that permits applications in high-speed optical communications. A nonlinear technique based on modulational instability of a pump wave induced by a small signal was first suggested by Hasegawa[2] and realized experimentally by Tai *et al.*[3] Another nonlinear method is based on the reshaping of a beat signal as a result of the superposition of two pump waves of equal power. Indeed, the nonlinear reshaping of the beat signal into well-separated short pulses was previously demonstrated by use of several methods based on dispersion-decreasing fibers,[4] the soliton Raman self-scattering effect in dispersion-decreasing fibers,[5] and switching in a nonlinear fiber loop mirror.[6] Other techniques based on steplike and comblike dispersion profiled fiber, using segments of conventional fibers with different dispersion, have also been proposed for the generation of picosecond and subpicosecond pulse trains with high repetition rates.[7–13] But the above-mentioned techniques have as a common feature that they require careful control of the chromatic dispersion along the propagation distance, thus leading to relatively complicated fiber systems. An alternative approach, based on multiple four-wave mixing (FWM) in an optical fiber with anomalous constant dispersion, was demonstrated theoretically for the generation of compressed pulse trains from the propagation of a dual-frequency pump field.[14] Relatively large compression ratios have thus been predicted theoretically, but the compressed pulses were accompanied by a strong pedestal component.[14] The objective of this Letter is to present what is believed to be the first experimental demonstration of generation of a transform-limited (TL) pedestal-free pulse train with a high repetition rate by means of the technique of multiwave mixing temporal compression in a standard nonzero dispersion-shifted fiber (NZ-DSF). In particular, in our experiments a 160-GHz train of 1.27-ps TL pedestal-free Gaussian pulses was obtained at 1550 nm by use of a single piece of 1-km-long NZ-DSF in the anomalous-dispersion regime. The technique of frequency-resolved optical gating (FROG), adapted for high-repetition-rate periodic pulse trains,[15,16] was used to characterize directly the intensity and the phase of the 160-GHz pulse train.

The initial beat signal was obtained by simultaneous injection of two linearly polarized continuous waves with different frequencies and equal powers into the NZ-DSF. We analyzed the nonlinear propagation of such a beat signal numerically with the split-step Fourier method to solve the generalized nonlinear Schrödinger equation,[17] including fiber loss and higher-order effects such as third-order dispersion, self-steepening, and intrapulse Raman scattering. Figure 1(a2) shows the 160-GHz sinusoidal input signal at 24-dBm average power evolving into compressed pulse train with ~1.3-ps FWHM pulses. The optimum fiber length for achievement of maximum compression with minimum chirp and pedestal was found to be $L = 2375$ m. At the central wavelength of the initial beat signal, i.e., $\lambda = 1550.35$ nm, the fiber is assumed to have 0.21 dB/km loss, an anomalous dispersion of 1 ps/nm km, a nonlinear coefficient of 1.7 W^{-1} km^{-1}, a Raman response time of 3 fs, and a third-order dispersion of 0.07 ps/nm^2 km. These parameters are those of the NZ-DSF used in our experiments. Figure 1(a1) shows that the phase across the pulses is constant, which implies that the compressed pulses are TL. The phase difference between two consecutive pulses is π. The pulse shape corresponds essentially to a Gaussian profile with 1.34-ps FWHM. The peaks of the spectral lines of the output spectrum, shown in Fig. 1(a3), were fitted by a continuous Gaussian envelope with a FWHM bandwidth of 0.32 THz, giving a time–bandwidth product of 0.43, very close to the value of 0.441 corresponding to TL Gaussian pulses. The compression efficiency may be enhanced by an increase in the average input power, as shown in Fig. 1(b2) for 30 dBm and $L = 977$ m. As

0146-9592/02/191729-03$15.00/0

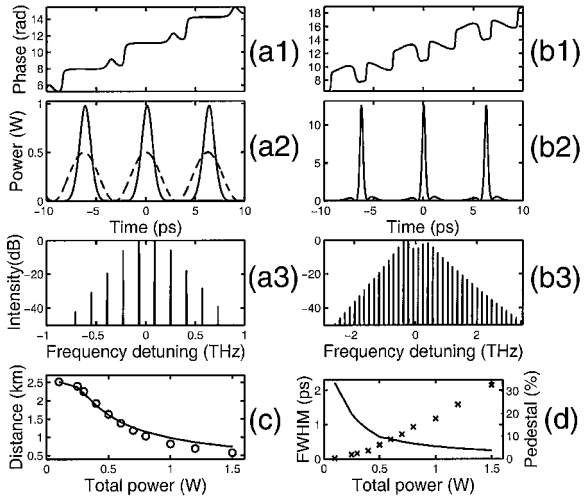

Fig. 1. Results of numerical simulation of transformation of a beat signal into a train of short pulses for an input average total power of 24 dBm (0.25 W). (a1) Phase variation. (a2) Intensity of the compressed pulse train (solid curve) and the input beat signal (dashed curve). (a3) Spectrum of the compressed pulse train. (b1), (b2), and (b3) Results of the pulse-train compression with an input average power of 30 dBm (1 W). (c) Optimum length versus the input total power. (d) Output pulse width (solid curve) and proportion of pedestal energy (×).

can be clearly seen from this figure, the compression efficiency is increased (FWHM, 364 fs), but meanwhile the quality of the pulse train is degraded as a result of the appearance of broad low-intensity pedestal components and a nonuniform phase across the pulses [see Fig. 1(b1)]. To describe the qualitative compression dynamics in more detail, we plot in Fig. 1(c) and 1(d) the evolution with input total power of the optimum propagation distance [solid curve in 1(c)] and both the output pulse width and the proportion of pedestal energy contained in the output pulse at the optimum fiber length. As can be clearly seen from Figs. 1(c) and 1(d), as the input power increases, the necessary optimum fiber length and output pulse width decrease, and the pulse quality is more and more degraded, since the pedestal energy continuously increases. Therefore, we verify that pedestal-free compression is possible only at low power. However, Fig. 1(c) shows that the optimum length can be accurately estimated over a wide range of input powers by calculation of the length at which the maximum conversion from the two initial pumps into the first-order sidebands occurs (open circles), thus confirming the validity of the four-mode analytical model proposed by Trillo *et al.*[14] Therefore, numerical solutions of the generalized nonlinear Schrödinger equation show that there exists a trade-off among pulse quality, average power, pulse width, and fiber length.

For the experimental demonstration of this technique, we focused our attention on the generation of TL pedestal-free pulses at a 160-GHz repetition rate. Figure 2 shows the design of the experimental setup. A dual-frequency beat signal was synthesized from two cw 150-kHz-linewidth tunable-wavelength external-cavity lasers. The center wavelength was fixed at $\lambda = 1550.35$ nm, and the zero-dispersion wavelength of the NZ-DSF was $\lambda_{ZD} = 1536.5$ nm. Both waves were combined by a fiber fused 50:50 coupler and then amplified to the desired average power level by an erbium-doped fiber amplifier. Stimulated Brillouin scattering was suppressed by external modulation of the two external-cavity lasers with a $LiNbO_3$ phase modulator. A 95:5 coupler placed at the amplifier output allowed for real-time monitoring of the stimulated Brillouin scattering signal. The two signal powers were set to the same value, and the polarization states were parallel aligned. The beat-signal power injected into the 1-km-long NZ-DSF was set to 27.2 dBm, which led to optimum compression with minimum pedestal. The output field after nonlinear reshaping in the NZ-DSF was characterized with an optical spectrum analyzer, a background-free second-harmonic-generation autocorrelator, and a FROG setup based on the spectral analysis of the second-harmonic-generation autocorrelation signal with the OSA. The FROG trace was conveniently built up by adjustment of the autocorrelator to a particular delay, and then the OSA wavelength was scanned. The measured temporally modulated spectra were then interpolated onto a 128 × 128 grid and used as input to the vector-based principal-components generalized projections algorithm for the retrieval of the periodic pulse-train characteristics.[15,16]

Figures 3(a) and 3(b) show the measured and retrieved second-harmonic-generation FROG traces of the field, respectively, after propagation through the 1-km NZ-DSF. The FROG trace exhibits a

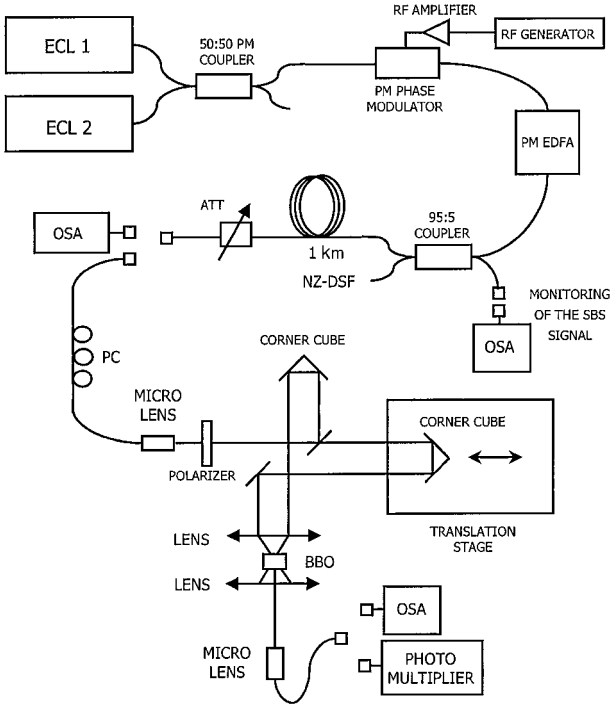

Fig. 2. Schematic of the experimental setup: ECL 1, ECL 2, external-cavity lasers; PM, polarization-maintaining; EDFA, erbium-doped fiber amplifier; ATT, variable attenuator; PC, polarization controllers; OSA's optical spectrum analyzers; BBO, β-barium borate; SBS, stimulated Brillouin scattering.

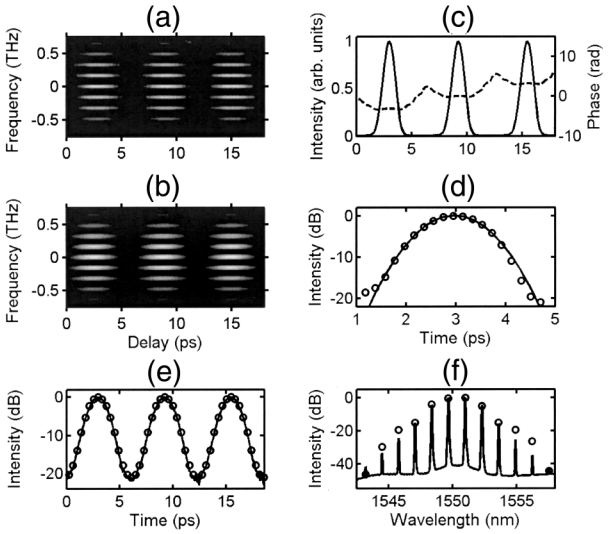

Fig. 3. (a) Measured and (b) retrieved SHG-FROG traces of the generated pulse train at 160 GHz. (c) Solid curve, retrieved intensity (left-hand axis); dashed curve, retrieved phase (right-hand axis). (d) Least-squares fit of the retrieved pulse shape (open circles) by a Gaussian function (solid curve). (e) Measured autocorrelation and (f) spectrum of the pulse train at fiber output (solid curves). The open circles show the autocorrelation and the spectrum calculated from the retrieved intensity and phase.

complex structure because of the generation of multiple four-wave mixing sidebands associated with the reshaping of the injected beat signal. The retrieval error, defined as the rms between the original and retrieved FROG traces, was found to be $G = 0.0035$. The corresponding retrieved intensity and phase are shown in Fig. 3(c). Remarkably, the intensity profile shows a reshaped pulse train that clearly has no pedestal. The phase variation over the compressed pulses forming the train is also negligibly small, indicating that the pulses are essentially TL. The phase difference between two consecutive pulses is π, in good agreement with theoretical predictions of Fig. 1. The solid curve in Fig. 3(d) is the least-squares fit of a Gaussian function to the retrieved pulse shape. As can be clearly seen from this figure, the intensity profile corresponds very well to a Gaussian function with 1.27-ps FWHM and 2.4-W peak power. The extinction ratio between peak power and interpulse background is better than 20 dB. As shown on a logarithm scale in Figs. 3(e) and 3(f), respectively, the autocorrelation and the spectrum that were derived from the retrieved pulse train are in excellent agreement with the independent direct experimental measurements, thus confirming the reliability of the experimental setup. Our experimental results are qualitatively in good agreement with the numerical solutions of the generalized nonlinear Schrödinger equation as shown in Fig. 1. However, a more direct comparison between theory and experiments would require perfect knowledge of the fluctuation of the physical parameters, such as dispersion, nonlinearity, and birefringence, along fiber length.

In conclusion, we have presented an experimental demonstration of highly efficient multiwave mixing compression of a sinusoidal beat signal into a high-quality train of Gaussian 1.27-ps TL pedestal-free pulses at a 160-GHz repetition rate and 1550 nm. The FROG technique was proved to be a powerful tool for accurately characterizing the intensity and phase of the 160-GHz pulse train. For an industrial application of this technique, the timing jitter that originates from fluctuations of frequency difference between the two light sources can be reduced by stabilization of the two external-cavity lasers through a single reference cavity, such as a Fabry–Perot resonator with very high finesse.[18] Finally, we believe that the very simple experimental technique described in this Letter exhibits great potential as a high-quality source of TL ultrashort pulses, which can be helpful for optimizing ultrahigh-bit-rate transmission lines.

Guy Millot's e-mail address is Guy.Millot@u-bourgogne.fr.

References

1. T. Yamamoto, E. Yoshida, K. R. Tamura, K. Yonenaga, and N. Nakazawa, IEEE Photon. Technol. Lett. **12,** 353 (2000).
2. A. Hasegawa, Opt. Lett. **9,** 288 (1984).
3. K. Tai, A. Tomita, J. L. Jewell, and A. Hasegawa, Appl. Phys. Lett. **49,** 236 (1986).
4. P. V. Mamyshev, S. V. Chernikov, and E. M. Dianov, IEEE J. Quantum Electron. **27,** 2347 (1991).
5. S. V. Chernikov, D. J. Richardson, R. I. Laming, E. M. Dianov, and D. N. Payne, Appl. Phys. Lett. **63,** 293 (1993).
6. S. V. Chernikov and J. R. Taylor, Electron. Lett. **29,** 658 (1993).
7. S. V. Chernikov, J. R. Taylor, and R. Kashyap, Electron. Lett. **29,** 1788 (1993).
8. S. V. Chernikov, J. R. Taylor, and R. Kashyap, Electron. Lett. **30,** 433 (1994).
9. S. V. Chernikov, J. R. Taylor, and R. Kashyap, Opt. Lett. **19,** 539 (1994).
10. S. V. Chernikov, R. Kashyap, M. J. Guy, D. G. Moodie, and J. R. Taylor, Philos. Trans. R. Soc. London Ser. A **354,** 719 (1996).
11. E. A. Swanson and S. R. Chinn, IEEE Photon. Technol. Lett. **7,** 114 (1995).
12. A. Maruta, Y. Yamamoto, S. Okamoto, A. Suzuki, T. Morita, A. Agata, and A. Hasegawa, Electron. Lett. **36,** 1947 (2000).
13. M. Tadakuma, O. Aso, and S. Namiki, in *Optical Fiber Communication Conference (OFC)*, postconference digest, Vol. 37 of OSA Trends in Optics and Photonics Series (Optical Society of America, Washington, D.C., 2000), pp. 178–180.
14. S. Trillo, S. Wabnitz, and T. A. B. Kennedy, Phys. Rev. A **50,** 1732 (1994).
15. F. Gutty, S. Pitois, P. Grelu, G. Millot, M. D. Thomson, and J. M. Dudley, Opt. Lett. **24,** 1389 (1999).
16. J. M. Dudley, F. Gutty, S. Pitois, and G. Millot, IEEE J. Quantum Electron. **37,** 587 (2001).
17. G. P. Agrawal, *Nonlinear Fiber Optics*, 3rd ed. (Academic, New York, 2001).
18. A. Schoof, J. Grünert, S. Ritter, and A. Hemmerich, Opt. Lett. **26,** 1562 (2001).